Phosphorene Edge Reconstruction by Self-Rolling

Junfeng Gao, Xiangjun Liu, Gang Zhang*, and Yong-Wei Zhang*

Institute of High Performance Computing, A*STAR, Singapore, 138632, Singapore

ABSTRACT. Edge atomic configuration often plays an important role in dictating the properties of finite-sized two-dimensional (2D) materials. Due to the presence of possible complex reconstructions and also the difficulties in experimental imaging, it remains unclear what is the most energetically stable configuration for phosphorene zigzag (zz) edge. By performing ab initio calculations, we identify a highly stable zz edge reconstruction of phosphorene among all the considered edges. Surprisingly, this highly stable edge exhibits a novel nanotube-like structure, which is topologically distinctively different from any previously reported edge reconstruction. We further show that this new edge type can form easily, with an energy barrier of only 0.234 eV, and it may be the dominant edge type at room temperature in vacuum condition or even under low hydrogen gas pressure. Importantly, the calculated electronic properties are consistent with recent experimental measurements. It is expected that this newly found edge structure may spark a re-visit to the various properties of finite-size phosphorene, stimulate more studies in uncovering other novel edge types, and further exploring their practical applications.

KEYWORDS. Phosphorene, edge stability, edge reconstruction, electronic properties.

1. Introduction

Phosphorene, a single-layer of black phosphorus, which possesses a puckered honeycomb lattice, has recently experienced a surge of research interest.[1, 2] Since its lattice structure is highly anisotropic, its mechanical, thermal and electronic properties are also highly anisotropic.[3, 4] In particular, it was shown[5] that phosphorene is a semiconductor with a direct band gap of ~2.0 eV, and exhibits an on-off current ratio above 10^5. In addition, the electronic properties of black phosphorus can be efficiently tuned via the number of layers, surface doping, strain and electronic field.[6-8] Evidently, phosphorene possesses many remarkable properties ideal for electronic and optoelectronic device applications.

Just like a surface is an integral part of any finite-size three-dimensional materials, an edge is an integral part of a finite-size two-dimensional (2D) material.[9-13] It was shown that edge states in graphene nanoribbons exhibit electronic properties distinctively different from the bulk states,[14-16] such as spin-dependent gapless chiral edge states[14] and pseudo-Landau levels[15]. Similarly, edge states can also have strong effect on the electronic properties of phosphorene. For example, previous theoretical studies revealed that phosphorene nanoribbons (PNRs) with pristine armchair (ac) edges are semiconducting,[17, 18] while PNRs with pristine zigzag (zz) edges are metallic[19-21]. In general, a pristine edge with unsaturated dangling bonds is unstable, leading to the atomic reconstruction of the edge. In 2D honeycomb lattices, due to the short distance of unsaturated dangling bonds at ac edges, a simple edge reconstruction by forming triple bonds in the armrests can easily lower the edge energy.[9, 10] For zz edges, however, the distance between two dangling bonds are too far to form any triple bonds. Therefore, to enhance the stability of zz edges, a complex reconstruction is often required. For example, by transforming two hexagons into a pentagon and a heptagon, pristine graphene zz edge can transform into the well-known

Haeckelite zz(57) edge, reducing the energy by ~2.1 eV/nm.[9] For transition metal dichalcogenides (TMDs), metal-terminated edges preferably undergo a unique (2×1) reconstruction by pushing half second-row halogens atoms outwards, causing, for example, an energy reduction of ~0.4 eV/nm for MoS_2, ~1.0 eV/nm for $MoSe_2$, ~1.2 eV/nm for WS_2 and ~1.4 eV/nm for WSe_2.[22] Compared to the extensive studies on the reconstruction of zz edges in graphene and TMDs,[9-12, 22] the study on the reconstruction of phosphorene zz edges remains rather limited. Due to the difficulties in directly imaging the edge structures experimentally, how a pristine phosphorene zz edge reconstructs itself remains unknown. Importantly, what is the most energetically stable configuration of zz phosphorene edges remains unclear.

In this Letter, we systemically study the stabilities and probable reconstructions of both zz and zz(Klein)[23] (zz(K)-type) edges, and their influence on the electronic properties via density functional theory (DFT) calculations. Surprisingly, we reveal a new form of 2D edge that is terminated by a nanotube structure by an easily self-rolling process. Compared with pristine zz edge, ***the nanotube-terminated edge is able to reduce the edge energy by 35%***. Importantly, it possesses the lowest edge energy among all the edge types explored, suggesting that this unique edge type may be present in reality. We further discuss experimental evidences that support our finding. It is expected that the finding of this new form of edge structure may also inspire more efforts to look for other novel forms of edge structures, and their applications.

2. Theory and computational methods

All first-principles calculations were performed by the VASP.[24] The PBE functional[25] and PAW method[26] were used to describe the exchange-correlation functional and core electrons, respectively. DFT-D3 correction of Grimme was used to calculate the vdW interaction.[27] The

kinetic energy cutoff was taken as 400 eV and the k-mesh was carefully tested (See the Supporting Information). The force criterion for structure optimization and climbing image nudged elastic band (cNEB) calculation[28] were taken both as 0.02 eV/Å. A very dense (20×1×1) k-mesh was used for the band structure calculations and STM simulations. In previous studies, all the zz edge atoms were considered to be equivalent.[19, 20, 29] Consequently, such treatment is unable to consider the edge reconstruction. In the present work, we employ a unit cell containing two periods along the edge for studying the edge reconstruction. Here, we focus on both pristine zz and zz(K)-type edges and their various reconstructed edge structures.

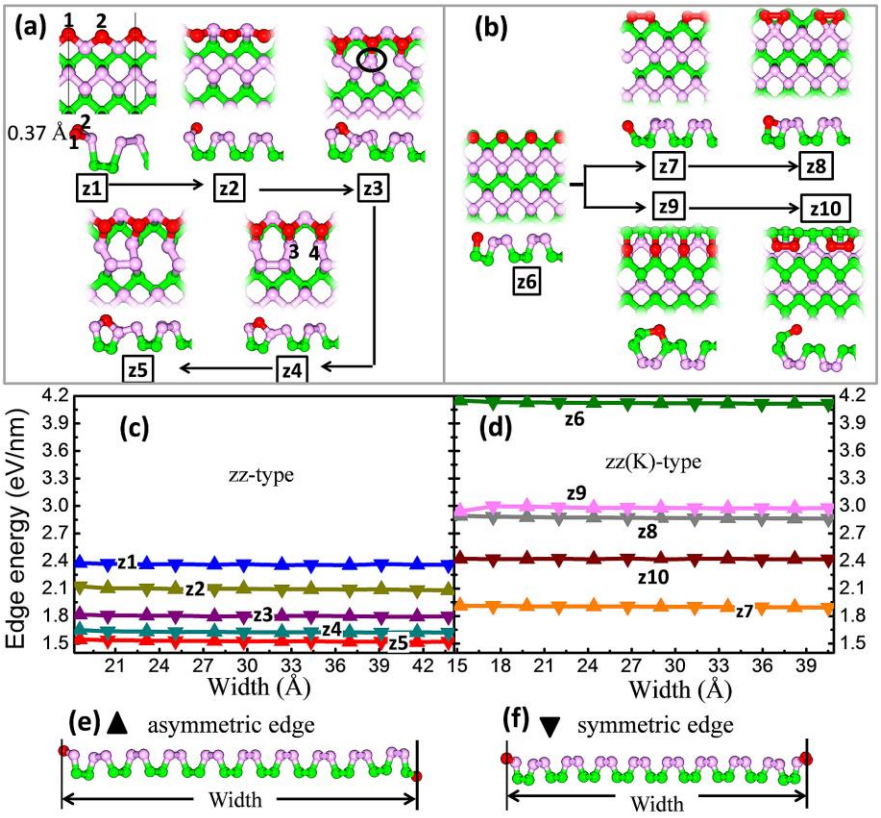

Figure 1. Possible zz-type (a) and zz(K)-type (b) edge structures and their edge energies (c)-(d), respectively. Side view of asymmetric (e) and symmetric (f) PNRs with the pristine z1 configuration. The definition of the width of PNR is also shown in (e) and (f).

3. Results and discussion

3.1 Tube-terminated edge reconstruction

Figure 1a shows the reconstruction process of pristine zz edge. It is seen that a spontaneous (2×1) reconstruction (z1 configuration) for pristine zz edge occurs first. In this process, the neighboring edge atoms (labeled by 1 and 2) undergo a 0.37 Å buckling in height and 0.21 Å shifting vertical to the edge. The edge atoms (red) of z1 are bent upwards with a displacement of 0.37~0.74 Å with reference to the inner P atoms. Subsequently, a series of edge conformation changes take place through bond bending and rolling (see the z1 to z4 configurations in Figure 1a). Eventually, a novel edge structure terminated by a nanotube (the z5 configuration) is formed.

To quantitatively understand the energetics during the above edge reconstruction of pristine zz edge, we calculated their edge energy per length γ using[9, 12]:

$$\gamma = \frac{1}{2L}(E_{PNR} - N_P E_P) \quad (1)$$

where E_{PNR} is the total energy of a PNR, N_P and E_P are the number of P atoms in the PNR and the energy of P atom in perfect phosphorene, respectively. L is the length of the PNR and the factor 2 accounts for the two edges of the PNR. Due to the puckered structure, a PNR can have two edges either in asymmetry (Figure 1e) or symmetry (Figure 1f). To exclude the interaction of two edges and achieve accurate edge energies, we have calculated the edge energy of a PNR with consecutively increasing its width over 43 Å. Here, the widths are defined as the width of pristine zz edge before reconstruction (Figure 1e, 1f).

Figure 1c shows the edge energy versus the PNR width, in which triangles (inverted triangles) represent the asymmetric edges (symmetric edge). It is seen that the edge energy is neither dependent on the width, nor the nature of edge symmetry. The edge energy of the (2×1) reconstructed z1 configuration is 2.36 eV/nm, which is slightly lower than pristine zz edge

(~0.08 eV/nm). Simply through flipping, the outward z1 configuration is able to transform into the inward z2 configuration. This process reduces the edge energy by 0.28 eV/nm (~11.8%). A further bending motion is able to connect the edge atom to the inner atoms in the same layer, and transform the z2 configuration into the z3 configuration. Since the z3 configuration eliminates the unsaturated bonds, its edge energy is reduced to only 1.80 eV/nm, giving rise to a 23.7% reduction.

It is noted that there are 4-coordinated P atoms (labeled by the black circle in Figure 1a) in the z3 configuration. Upon a reallocation of P-P bonds, a higher-symmetry z4 configuration with all 3-coordinated P atoms is formed. In this process, the edge energy is reduced to ~1.62 eV/nm. The energy of z4 configuration can be further reduced by changing the orientation of the opposite lone pair electrons of atom-3 and atom-4 to eliminate the repelling interaction between them. This process transforms the z4 configuration into the nanotube-terminated z5 configuration. The edge energy of the z5 configuration is 1.52 eV/nm, which is only 64.4% of the z1 configuration. Clearly, among all the edges in the reconstruction process, the nanotube terminated z5 configuration possesses the lowest edge energy.

Figure 1b (1d) shows the structures (edge energy) of pristine and reconstructed zz(K) edges. The edge energy of pristine zz(K) edge (the z6 configuration) is 4.11 eV/nm, which is the highest in all our explorations. Upon energy relaxation, the z6 configuration is able to transform into the (2×1) reconstructed z7 configuration, which is similar to the previously reported graphene zz(K) edge[9, 12]. However, different from the high instability of graphene zz(K) edge, the edge energy of the reconstructed z7 configuration is only 1.89 eV/nm, which is 0.47 eV lower than the (2×1) reconstructed z1 configuration (Figure 1c). In addition, we also examine three other reconstructed edges of the zz(K) edges, that is, the z8, z9 and z10 as shown in Figure 1b. The z8

configuration can be obtained by bending the edge atoms to form a small tube. The z9 configuration can be obtained by rolling up edge atoms to form a large tube. By opening up the nanotube in the z9 configuration, the z10 configuration can be obtained. Our calculations also show that the edge energy of the z8, z9 and z10 configurations is 0.97 eV/nm, 1.09 eV/nm and 0.53 eV/nm higher than that of the z7 configuration, respectively. Therefore, the z7 configuration is the most stable zz(K)-type edge. However, its edge energy is still 0.37 eV/nm (19.6%) higher than the z5 edge. Hence, our calculations suggest that the z5 configuration is the most energetically stable, and thus should be the dominated edge in terms of thermal stability. It is noted that the z8 configuration was used to explain the observed semiconducting behavior of PNRs in scanned tunneling spectrum.[30] However, our results show that the high energy of the z8 configuration will limit its occurrence in reality.

3.2 Transition pathway and energy barrier

In the above analysis, we have revealed surprisingly that the zz edges of PNRs can be terminated by nanotubes. In the following, we examine the transition pathway and related energy barriers from the z1 to z5 edge configurations (Figure 2a) using 6-unit PNRs supercell along the edge. The change in the total energy was plotted in Figure 2c, and the transitions and intermediate structures for the first two edge atoms were shown in Figure 2a (a1-a5 in the yellow zone of Figure 2c, and also the whole movie-S2).

Overall, the z5 configuration is about 1.577 eV lower than the initial z1 configuration in the supercell, implying a strong driving force for the evolution. The tube formation starts with a pair of adjacent edge atoms and then propagates along the edge in a clear stepwise manner with two adjacent edge atoms as a unit. The transition pathway and corresponding energy evolution for the first pair of edge atoms are shown in Figure 2a and Figure 2c, respectively. Initially, the two

adjacent edge atoms roll up by overcoming an energy barrier of 0.474 eV (from a1 to a2) to reach the intermediate state (a3). Then, by overcoming a small barrier of 0.035 eV (from a3 to a4), the edge state a5 is formed, which is 0.35 eV lower than that of the a1 state. Subsequently, the adjacent two edge atoms begin to roll up and repeat the similar reconstruction behavior as the first pair. The flipping barrier for the second pair is 0.439 eV, which is 0.035 eV lower than that of the first pair. For the third pair, the flipping barrier further decreases to 0.387 eV, implying that the subsequent flipping barrier may be monotonically decaying.

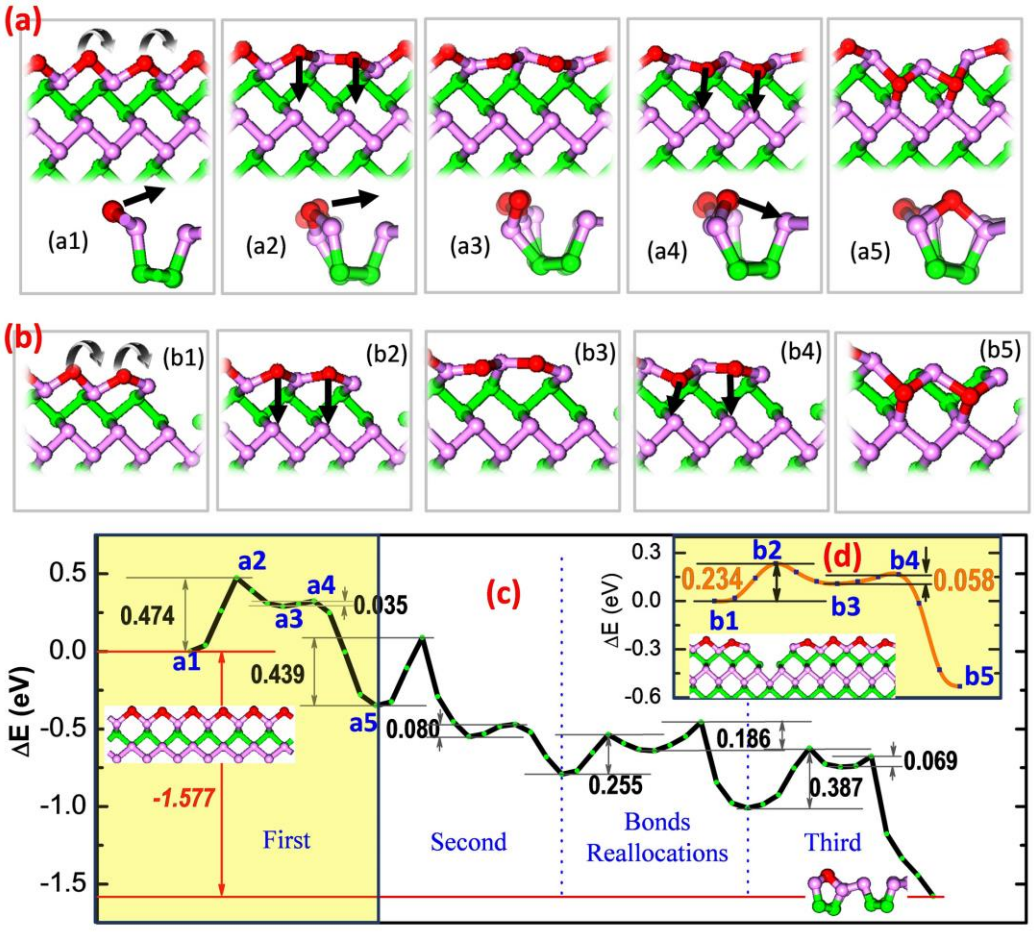

Figure 2. Reconstruction process from the pristine z1 configuration to the tubed z5 configuration. (a) a series of structure transformation in the reconstruction of the flat zz edge, (b) the consecutive transition structures for the zz edge with a kink, (c) the transition pathway and

related energy changes from the flat z1 edge to the tubed z5 edge, and (d) the transition pathway and related energy changes starting from a kink site of the zz configuration.

During the roll-up of edge atoms, there are some consecutive P-P bond reallocations, corresponding to the change from z3 to z5 configuration. As shown in Figure 2c, the reallocation barriers (0.255 eV and 0.186 eV) are much lower than the flipping barriers. This is in consistent with the easy reallocation of inner P-P bonds observed in previously *ab initio* molecular simulation of phosphorene nanoflake[31] and the low barrier of defect diffusion in phosphorene[32]. Overall, the highest energy barrier arises from the roll-up of edge atoms, especially for the first pair (0.474 eV). Thus we can estimate the average edge transition rate $\boldsymbol{R}$ by:

$$\boldsymbol{R} \sim (\frac{k_B T}{h}) \times exp(-\Delta E/k_B T) \quad (2)$$

where T is the temperature, k_B and h are the Boltzmann and Plank constants, respectively. ΔE=0.474 eV. At room temperature (300K), the average edge transition rate $\boldsymbol{R}$ is about 10^5 Hz. Besides, at elevated 400 K, $\boldsymbol{R}$ reaches to 10^6 Hz. At the thermal decomposition temperature ~400 ^{o}C,[33] the average edge transition is 10^9 Hz, indicating that the edge transition will happen in just several nanoseconds at this temperature.

In general, an edge atomic structure may be not perfect. Our DFT calculation shows that the formation energy of a kink (the inset structure in Figure 2d) along the edge is only 0.22 eV/atom. The possibility to form a kink along the edge is $e^{(-\frac{0.22\ eV}{k_B T})}$, which is ~$10^{-4}$ at 300 K. Thus, there should be a kink in the micrometer scale. In reality, the density of kink along the edge could be even higher.[30]

We then investigate the effect of kink on the edge reconstruction. Figure 2b and 2d show the transition structures and energy barriers for the roll-up of the first pair of two adjacent edge atoms near the kink. Although the transition processes are very similar to those of the regular z1

edge, the highest flipping barrier is reduced to 0.234 eV, which is only half of the regular edge (0.474 eV). Taking edge kink into account, the average edge transition rate increases to 10^9 Hz at 300 K. According to previous *ab initio* molecular dynamics simulation, the tubed configuration can be formed in the picosecond scale at the edge corner of phosphorene nanoflake[31]. Therefore, it is expected that the tubed z5 configuration can be formed rapidly, and should be the dominated configuration even at room temperature.

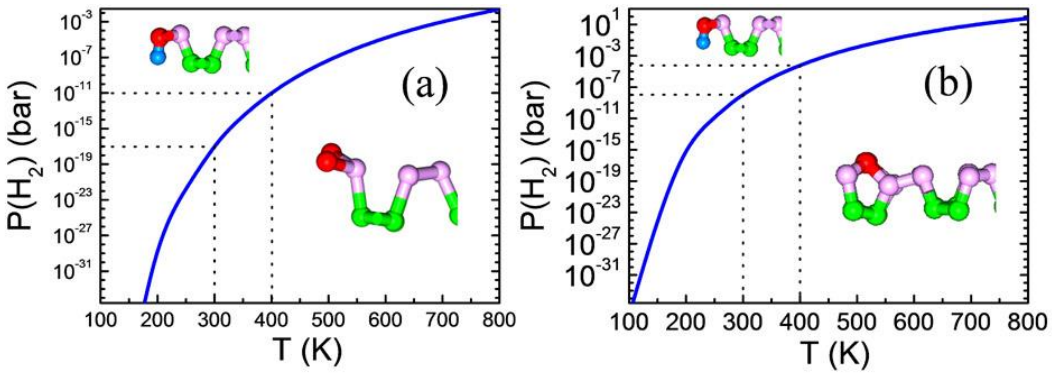

Figure 3. The phase diagram of the bare and hydrogenated zz edges under various temperatures and partial pressures of hydrogen gas. (a) the z1 edge vs. the zz-H edge; and (b) the tubed z5 edge vs. the zz-H edge.

3.3 Phase diagram analysis

Similar to graphene[10], the structure and stability of phosphorene edge may be greatly affected when exposed to H_2 gas[19, 34]. In the following, we compare the stability of z1, z5 and hydrogenated zz configurations. The edge energy γ(H) of hydrogenated zz edge can be calculated by[10]:

$$\gamma(H) = \frac{1}{2L}(E_{ribb} - N_P E_P - \frac{N_H}{2} E_{H_2}) \quad (3)$$

where E_{H_2} is the energy of a H_2 molecule obtained from DFT calculations. The γ(H) is about 0.18 eV/nm, which is slightly higher than the previous results since the DFT-D3 is adopted in our calculations. The change of Gibbs free energy associated with the related stability of hydrogenated edge with respect to the bare edge can be calculated by:

$$\Delta G = \gamma(H) - \frac{\rho_H}{2}\Delta\mu(H_2) \quad (4)$$

where ρ_H is the concentration of H atoms along the hydrogenated edge. At the absolute temperature T and under a certain partial pressure P(H_2), the chemical potential of H_2 gas is:

$$\Delta\mu(H_2) = H^0(T) - H^0(0) - TS^0(T) + k_B T ln[\frac{P(H_2)}{P_0}] \quad (5)$$

where the $H^0(T)$ and $S^0(T)$ can be obtained from the NIST-JANAF thermochemical tables,[35] the reference pressure is P_0=1 bar.

Figure 3 presents the phase diagram of the hydrogenated edge in comparison with the bare z1 edge (Figure 3a) and the tubed z5 edge (Figure 3b), respectively. It is seen that the bare z1 edge can only exist under very low H_2 pressure. At 300 (400) K, the z1 edge can only exist under an ultra-low H_2 pressure of 10^{-17} (10^{-11}) bar (Figure 3a). At lower temperature, the transition hydrogen pressure should be even lower.

As mentioned above, the z1 edge without hydrogenation will rapidly transform into the tubed z5 edge at room temperature and above. After this reconstruction, the chemical stability of the z5 edge is significantly enhanced. At room temperature, the transition pressure P(H_2) from the tubed z5 configuration to the hydrogenated zz configuration is ~10^{-8} bar, which is close to the H_2 partial pressure in air (~10^{-7} bar). At elevated temperature, the transition pressure P(H_2) is above the H_2 partial pressure in air. For example, at 400 K, the transition pressure P(H_2) is ~10^{-4} bar, which is three orders higher than the H_2 partial pressure in air at the same temperature. Usually, the production and fabrication of phosphorene are under high vacuum condition,[34, 36, 37] where

the hydrogen pressure is usually much lower than the partial pressure in air. Therefore, the most stable phosphorene edge should be the tubed z5 edge in the practical condition.

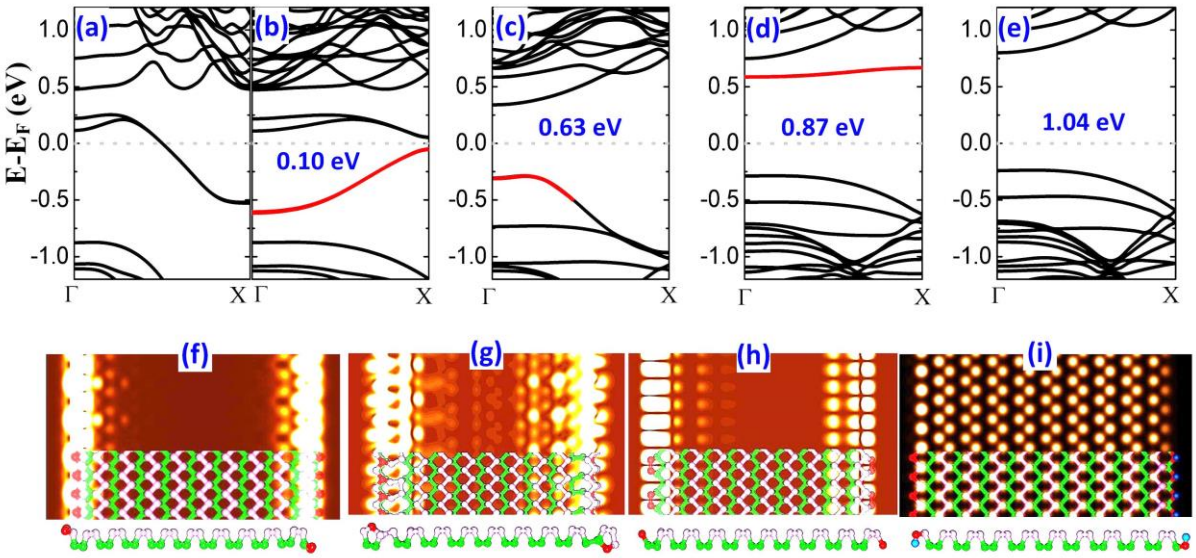

Figure 4. The band structures of PNRs with different edges. (a) the pristine zz edge; (b) the z1 edge; (c) the z5 edge terminated with a nanotube; (d) the z7 edge; and (e) the hydrogenated edge. The simulated STM images of the z1 edge at -0.7 V bias (f); the z5 edge at -0.5 V bias (g), the z7 edge at +0.7 V bias (h), and the hydrogenated zz edge at -1.5 V bias (i).

3.4 Electronic properties of various edges

Next we investigate the electronic properties of the pristine zz, (2×1) reconstructed z1, tubed z5, zz(K)-type z7 and hydrogenated zz edges using wide asymmetric PNRs. It should be noted that to suppress the reconstruction, the pristine zz edge includes only one periodic unit along the edge. The calculation results are shown in Figure 4. It is seen that the band structure of the pristine zz edge exhibits a clearly metallic character (Figure 4a), in agreement with previous calculations.[19-21] After (2×1) reconstruction, the PNR become a semiconductor with a narrow band gap of 0.10 eV (Figure 4b).

It is seen that the PNR with the tubed z5 edges possesses a band gap of 0.63 eV (Figure 4c), which is 0.53 eV larger than the reconstructed z1 edge. It is also seen that the edge state in band structure is close to the valence band. Therefore, the calculated band gap and the position of the edge state of the z5 edge are in good agreement with previous experimental measurements of phosphorene zz edges.[30]

We have shown that the z7 configuration is the lowest energy structure among all the zz(K) type edges, and therefore, it will prevent the formation of the previously proposed z8 edge.[30] We find that the z7 configuration also has a large band gap of 0.87 eV (Figure 4d). However, the edge state in the band gap of the z7 configuration is close to the conduction band, which is opposite to the scanned tunneling spectrum observed experimentally.[30] For the hydrogenated phosphorene edge, the band gap is 1.04 eV, which is nearly the same as the perfect phosphorene monolayer calculated using standard GGA. In addition, there is no edge state in the band gap (Figure 4e). Therefore, the good agreement with experimental measurement of the electronic properties further confirms that the tubed z5 configuration is the dominant edge under high vacuum condition.

Currently, it is still a significant challenge to experimentally resolve the fine edge structure due to the considerable height fluctuation near the edge. Besides, the high resolution signals can only be obtained at a small bias window related to the edge state position in the gap. To facilitate experimental observations, we simulate STM images of these typical edges. We find that there are large differences in the edge signals among the z1 (Figure 4f), the tubed z5 edge (Figure 4g) and the z7 edge (Figure 4h), under corresponding bias according to the red lines in their band structures, i.e. -0.7 V for z1, -0.5 V for z5 and +0.7 V for z7 edge. Note that even though we

have used -1.5 V bias for hydrogenated edge (Figure 4i), no significant edge state is found in the simulated STM images.

4. Conclusions

In summary, we have investigated various possible reconstructions for pristine phosphorene zz and zz(K) edges. Surprisingly, the most stable edge is found to be the one terminated by a nanotube configuration. Of practical interest is that this edge configuration can easily occur at room temperature, and is stable against hydrogenation even under common production and fabrication process of phosphorene. Furthermore, our calculations show that the electronic properties of the tube-terminated edge are consistent with previous experimental measurements. Finally, we have also provided the simulated STM images to facilitate experimental observation. It is expected that the compelling evidences presented here for the presence of the tube-terminated zigzag edge will stimulate more studies in finding other novel edge types, and further exploring their practical applications.

ASSOCIATED CONTENT

Supporting Information. The calculation tests for energy cutoff and k-mesh and the whole reconstruction processes from z1 edge to tube-terminated z5 edge (Movie-S2). This material is available free of charge via the Internet at http://pubs.acs.org.

AUTHOR INFORMATION

Corresponding Authors:

Gang Zhang: zhangg@ihpc.a-star.edu.sg

Yong-Wei Zhang: zhangyw@ihpc.a-star.edu.sg

NOTES

The authors declare no competing financial interest.

ACKNOWLEDGMENT

This work was supported in part by a grant from the Science and Engineering Research Council (152-70-00017). The authors gratefully acknowledge the financial support from the A*STAR, Singapore and the use of computing resources at the A*STAR Computational Resource Centre, Singapore.

ABBREVIATIONS

2D, two-dimensional; zz, zigzag; PNRs, phosphorene nanoribbons; ac, armchair; TMDs, transition metal dichalcogenides; zz(K), zz(Klein); DFT, density functional theory; VASP, Vienna Ab-initio Simulation Package; PBE, Perdew–Burke–Ernzerhof; PAW, projector augmented wave; cNEB, climbing image nudged elastic band; GGA, generalized gradient approximation; STM, scanning tunneling microscope.

REFERENCES

(1) Liu, H.; Neal, A. T.; Zhu, Z.; Luo, Z.; Xu, X.; Tománek, D.; Ye, P. D. Phosphorene: An Unexplored 2D Semiconductor with a High Hole Mobility. *ACS Nano* **2014,** *8*, 4033-4041.

(2) Li, L.; Yu, Y.; Ye, G. J.; Ge, Q.; Ou, X.; Wu, H.; Feng, D.; Chen, X. H.; Zhang, Y. Black phosphorus field-effect transistors. *Nat. Nano.* **2014,** *9*, 372-377.

(3) Qiao, J.; Kong, X.; Hu, Z.-X.; Yang, F.; Ji, W. High-mobility transport anisotropy and linear dichroism in few-layer black phosphorus. *Nat. Commun.* **2014,** *5*, 4475.

(4) Cai, Y.; Ke, Q.; Zhang, G.; Feng, Y. P.; Shenoy, V. B.; Zhang, Y.-W. Giant Phononic Anisotropy and Unusual Anharmonicity of Phosphorene: Interlayer Coupling and Strain Engineering. *Adv. Funct. Mater.* **2015,** *25*, 2230-2236.

(5) Ling, X.; Wang, H.; Huang, S.; Xia, F.; Dresselhaus, M. S. The renaissance of black phosphorus. *Proc. Natl. Acad. Sci. U.S.A.* **2015,** *112*, 4523-4530.

(6) Cai, Y.; Zhang, G.; Zhang, Y.-W. Layer-dependent Band Alignment and Work Function of Few-Layer Phosphorene. *Sci. Rep.* **2014,** *4*, 6677.

(7) Kim, J.; Baik, S. S.; Ryu, S. H.; Sohn, Y.; Park, S.; Park, B.-G.; Denlinger, J.; Yi, Y.; Choi, H. J.; Kim, K. S. Observation of tunable band gap and anisotropic Dirac semimetal state in black phosphorus. *Science* **2015,** *349*, 723-726.

(8) Morgan Stewart, H.; Shevlin, S. A.; Catlow, C. R. A.; Guo, Z. X. Compressive Straining of Bilayer Phosphorene Leads to Extraordinary Electron Mobility at a New Conduction Band Edge. *Nano Lett.* **2015,** *15*, 2006-2010.

(9) Koskinen, P.; Malola, S.; Häkkinen, H. Self-Passivating Edge Reconstructions of Graphene. *Phys. Rev. Lett.* **2008,** *101*, 115502.

(10) Wassmann, T.; Seitsonen, A. P.; Saitta, A. M.; Lazzeri, M.; Mauri, F. Structure, Stability, Edge States, and Aromaticity of Graphene Ribbons. *Phys. Rev. Lett.* **2008,** *101*, 096402.

(11) Huang, B.; Liu, M.; Su, N.; Wu, J.; Duan, W.; Gu, B.-l.; Liu, F. Quantum Manifestations of Graphene Edge Stress and Edge Instability: A First-Principles Study. *Phys. Rev. Lett.* **2009,** *102*, 166404.

(12) Gao, J.; Zhao, J.; Ding, F. Transition Metal Surface Passivation Induced Graphene Edge Reconstruction. *J. Am. Chem. Soc.* **2012,** *134*, 6204-6209.

(13) Zhang, Z.; Liu, Y.; Yang, Y.; Yakobson, B. I. Growth Mechanism and Morphology of Hexagonal Boron Nitride. *Nano Lett.* **2016**, *16*, 1398–1403.

(14) Yao, W.; Yang, S. A.; Niu, Q. Edge States in Graphene: From Gapped Flat-Band to Gapless Chiral Modes. *Phys. Rev. Lett.* **2009,** *102*, 096801.

(15) Zhang, D.-B.; Seifert, G.; Chang, K. Strain-Induced Pseudomagnetic Fields in Twisted Graphene Nanoribbons. *Physical Review Letters* **2014,** *112*, 096805.

(16) Si, C.; Liu, Z.; Duan, W.; Liu, F. First-Principles Calculations on the Effect of Doping and Biaxial Tensile Strain on Electron-Phonon Coupling in Graphene. *Phys. Rev. Lett.* **2013,** *111*, 196802.

(17) Farooq, M. U.; Hashmi, A.; Hong, J. Manipulation of Magnetic State in Armchair Black Phosphorene Nanoribbon by Charge Doping. *ACS Appl. Mater. Interfaces* **2015,** *7*, 14423-14430.

(18) Peng, X.; Copple, A.; Wei, Q. Edge effects on the electronic properties of phosphorene nanoribbons. *J. Appl. Phys.* **2014,** *116*, 144301.

(19) Li, W.; Zhang, G.; Zhang, Y.-W. Electronic Properties of Edge-Hydrogenated Phosphorene Nanoribbons: A First-Principles Study. *J. Phys. Chem. C* **2014**, *118*, 22368.

(20) Guo, H.; Lu, N.; Dai, J.; Wu, X.; Zeng, X. C. Phosphorene Nanoribbons, Phosphorus Nanotubes, and van der Waals Multilayers. *J. Phys. Chem. C* **2014,** *118*, 14051-14059.

(21) Carvalho, A.; Rodin, A. S.; Neto, A. H. C. Phosphorene nanoribbons. *EPL (Europhysics Letters)* **2014,** *108*, 47005.

(22) Cui, P.; Choi, J.-H.; Chen, W.; Zeng, J.; Zhang, C.; Shih, C.-K.; Li, Z.; Zhang, Z. Distinct Reconstruction Patterns and Spin-Resolved Electronic States along the Zigzag Edges of Transition Metal Dichalcogenides. *arXiv:1511.04287 [cond-mat.mtrl-sci]* **2015**.

(23) Klein, D. J. Graphitic polymer strips with edge states. *Chem. Phys. Lett.* **1994,** *217*, 261-265.

(24) Kresse, G.; Furthmüller, J. Efficient iterative schemes for ab initio total-energy calculations using a plane-wave basis set. *Phys. Rev. B* **1996,** *54*, 11169-11186.

(25) Perdew, J. P.; Burke, K.; Ernzerhof, M. Generalized Gradient Approximation Made Simple. *Phys. Rev. Lett.* **1996,** *77*, 3865-3868.

(26) Blöchl, P. E. Projector augmented-wave method. *Phys. Rev. B* **1994,** *50*, 17953-17979.

(27) Grimme, S.; Antony, J.; Ehrlich, S.; Krieg, H. A consistent and accurate ab initio parametrization of density functional dispersion correction (DFT-D) for the 94 elements H-Pu. *J. Chem. Phys.* **2010,** *132*, 154104.

(28) Henkelman, G.; Uberuaga, B. P.; Jónsson, H. A climbing image nudged elastic band method for finding saddle points and minimum energy paths. *J. Chem. Phys.* **2000,** *113*, 9901-9904.

(29) Ramasubramaniam, A.; Muniz, A. R. *Ab initio* studies of thermodynamic and electronic properties of phosphorene nanoribbons. *Phys. Rev. B* **2014,** *90*, 085424.

(30) Liang, L.; Wang, J.; Lin, W.; Sumpter, B. G.; Meunier, V.; Pan, M. Electronic Bandgap and Edge Reconstruction in Phosphorene Materials. *Nano Lett.* **2014,** *14*, 6400-6406.

(31) Gao, J.; Zhang, G.; Zhang, Y.-W. The Critical Role of Substrate in Stabilizing Phosphorene Nanoflake: A Theoretical Exploration. *J. Am. Chem. Soc.* **2016,** *138*, 4763–4771.

(32) Hu, W.; Yang, J. Defects in Phosphorene. *J. Phys. Chem. C* **2015,** *119*, 20474-20480.

(33) Liu, X.; Wood, J. D.; Chen, K.-S.; Cho, E.; Hersam, M. C. In Situ Thermal Decomposition of Exfoliated Two-Dimensional Black Phosphorus. *J. Phys. Chem. Lett.* **2015,** *6*, 773-778.

(34) Xihong, P.; Qun, W. Chemical scissors cut phosphorene nanostructures. *Mater. Res. Express* **2014,** *1*, 045041.

(35) Chase, M. W.; Jr. et al., *NIST-JANAF Thermochemical Tables,*. American Institute of Physics: New York, 1998.

(36) Favron, A.; Gaufres, E.; Fossard, F.; Phaneuf-Lheureux, A.-L.; Tang, N. Y. W.; Levesque, P. L.; Loiseau, A.; Leonelli, R.; Francoeur, S.; Martel, R. Photooxidation and quantum confinement effects in exfoliated black phosphorus. *Nat. Mater.* **2015,** *14*, 826-832.

(37) Joshua, O. I.; Gary, A. S.; Herre, S. J. v. d. Z.; Andres, C.-G. Environmental instability of few-layer black phosphorus. *2D Mater.* **2015,** *2*, 011002.